
PERFORMATIVE DRIFT RESISTANT CLASSIFICATION USING GENERATIVE DOMAIN ADVERSARIAL NETWORKS

Maciej Makowski, Brandon Gower-Winter, Georg Krempf

Utrecht University

8 Hiedelberglaan, Utrecht, 3584 CS, NL

m.w.makowski@students.uu.nl, b.gower-winter@uu.nl, g.m.krempf@uu.nl

ABSTRACT

Performative Drift is a special type of Concept Drift that occurs when a model’s predictions influence the future instances the model will encounter. In these settings, retraining is not always feasible. In this work, we instead focus on drift understanding as a method for creating drift-resistant classifiers. To achieve this, we introduce the Generative Domain Adversarial Network (GDAN) which combines both Domain and Generative Adversarial Networks. Using GDAN, domain-invariant representations of incoming data are created and a generative network is used to reverse the effects of performative drift.

Using semi-real and synthetic data generators, we empirically evaluate GDAN’s ability to provide drift-resistant classification. Initial results are promising with GDAN limiting performance degradation over several timesteps. Additionally, GDAN’s generative network can be used in tandem with other models to limit their performance degradation in the presence of performative drift. Lastly, we highlight the relationship between model retraining and the unpredictability of performative drift, providing deeper insights into the challenges faced when using traditional Concept Drift mitigation strategies in the performative setting.

Keywords Concept Drift · Performative Prediction · Generative Neural Network · Domain Adversarial Neural Network · Drift Modeling

1 Introduction

Machine Learning has transformed decision-making across various domains. However, once deployed, models may encounter unforeseen factors that degrade performance by requiring the model to make predictions on data that originated from a distribution different to its training data. This phenomena is more broadly known as Concept Drift [1] and is most commonly associated with environmental factors that are intrinsic to the setting the predictive model is deployed in. Recently, a new type of drift has been identified that does not arise due to these intrinsic factors, but rather due to the presence of the predictive model embedded within the setting it is making predictions in. Such scenarios are described as Performative [2], and are identifiable by the causal relationship between the predictions a model makes and the drift the system experiences.

In such cases, performative drift can lead to dangerous feedback loops. For example, a company that struggles financially might face higher debt service costs (assigned by a predictive model) which, in turn, further engenders the company’s financial struggles. To combat Concept Drift generally, methods like retraining with new data or online learning exist [3] but they are not always sustainable, especially in the performative setting where model updates are likely to introduce additional or different performative drift phenomena that must be perpetually reacted to. An alternative approach would be drift understanding [4] whereby predictive models may be imbued with the ability to not only understand the drift they are experiencing, but adapt to it.

To achieve this goal, we propose a novel approach to handling model deterioration caused by performative drift. Leveraging domain adversarial neural networks (DANN) [5] and generative adversarial networks (GAN) [6, 7], our

architecture, GDAN, extracts domain-invariant features, enabling more robust classification, regardless of whether the data originates from the original training distribution or one altered by model predictions.

Our main contributions are the following:

1. The leveraging of drift understanding as a method for addressing performance degradation caused by performative drift.
2. A novel architecture (GDAN) that is drift-resistant and capable of simulating distribution shifts caused by performative drift.
3. We demonstrate why performative drift is unique when compared to intrinsic drift, and illustrate why traditional methods for handling Concept Drift (such as incremental learning) may prove ineffective in performative settings.

Lastly, we make the source code and Supplementary Materials for this paper available at: <https://tinyurl.com/erat3t47>

2 Background and Related Work

2.1 Performativity

If a setting is performative, a model’s predictions affect the data that it must later predict on. Performative drift is a model-dependent form of Concept Drift and is distinct from traditional (intrinsic) concept drift which is model-independent. The term performativity was introduced described by Perdomo et al. [2] when they introduced the concept of performative risk, a loss function that describes the performance degradation a model will experience when evaluated on future data distributions it engenders. They also introduced *repeated risk minimisation* (RRM), a procedure which repeatedly finds a model that minimizes the performative risk. Under strict assumptions, retraining in RRM can cause performative risk to converge, thus eliminating the need for model retraining.

Performativity has been discussed under various names in different domains. In the context of classification in data streams, the concept drift caused by this phenomenon has earlier been described as prediction-induced drift [8, 4]. Performativity has also been observed in Recommender Systems, which have to manage the performative effect recommendations have on the content consumed by their users [9, 10, 11]. Adversarial Learning is also inherently performative with adversaries updating their strategies in response to detectors which react and update their strategies in response to the adversaries [12, 13].

2.2 Domain Adversarial Neural Networks (DANNs)

Domain Adversarial Neural Networks (DANNs) [5] address domain adaptation by learning domain-invariant features that generalize across different data distributions. DANNs consist of three components: a feature extractor (F), a label predictor (LC), and a domain classifier (DC). The feature extractor aims to confuse the domain classifier by minimizing the following objective function:

$$E = \mathcal{L}_{LC} - \lambda \cdot \mathcal{L}_{DC} \quad (1)$$

Training involves a min-max game where LC minimizes \mathcal{L}_{LC} , while DC tries to minimize \mathcal{L}_{DC} and simultaneously maximize the overall objective.

2.3 Generative Adversarial Networks

Generative Adversarial Networks (GANs) [7] generate data resembling a given dataset by employing two neural networks: a generator (G) and a discriminator (D). The networks engage in a two-player min-max game, with the generator trying to produce fake samples $G(z)$ from noise $z \sim P(Z)$, while the discriminator tries to distinguish real data $x \sim P(X)$ from generated data. Training GANs can pose several challenges, such as training instability [14], undifferentiable outputs [15] and mode collapse. Standard GANs focus on distinguishing between real and fake data. Mirza et al. [16] enhanced this by conditioning the GAN on additional information, such as class labels, to generate more targeted outputs. Both the generator and discriminator receive extra inputs, enabling more controlled data generation. Building on this, Odena et al. [17] introduced the Auxiliary Classifier GAN (AC-GAN), where the discriminator outputs two probability distributions: one for real vs. fake classification and another for class prediction. Isola et al. [18] introduced a method for image-to-image translation using conditional GANs. The discriminator’s input

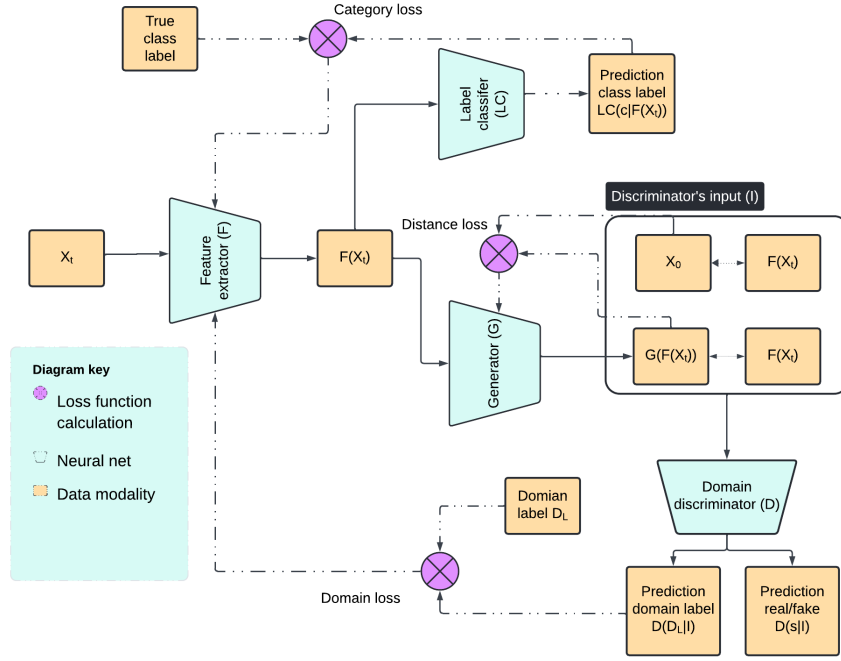


Figure 1: GDAN architecture, composed of a domain adversarial network and a generative adversarial network. Single-sided arrows illustrate an input/output relationship, while double-sided arrows describe concatenation of data.

is extended by pairing real data x with either target data y or generator outputs $G(x)$, enabling the generator to learn how to produce target images from x . To improve results, the L1 distance metric is used between the translated image and the target image [19].

3 GDAN - Generative Domain Adversarial Networks

This section presents GDAN, a performative drift resistant architecture that maps new distributions back to their original pre-drift distributions. The system integrates Domain Adversarial Neural Networks and Generative Adversarial Networks, employing necessary modifications to combine these concepts.

Figure 1 illustrates the architecture of the model. Here, X_t refers to a data point at iteration t . Each sample is represented as a tuple (X_t, D_t, c) . Where X_t is the set of attributes, D_t is the label of the distribution from which the point is sampled, and c is the class label. GDAN comprises of the following components:

- **Feature Extractor (F)**: Extracts domain-invariant features from X_t , making the output $F(X_t)$ generic and domain-independent.
- **Label Classifier (LC)**: Uses $F(X_t)$ to predict class c , ensuring robustness in classification despite distributional shifts caused by performative drift.
- **Generator (G)**: Maps non-domain-specific representations $F(X_t)$ back to the original distribution. G learns the nature of the drift from X_0 to X_t .
- **Discriminator (D)**: Input to the discriminator I consists of real data points paired with their domain-invariant representations $(X_t, F(X_t))$ split equally with generated data points paired with the corresponding representations used to generate said data points $(G(F(X_t)), F(X_t))$. D outputs two probability distributions: one indicating the origin of the data point (D_t) and the other assessing whether the point is from the real or generated distribution.

3.1 Objective

GDAN comprises of several components, all of which need to be considered when developing an objective function. First, consider the discriminator D . The loss of D is two-fold: L_s denotes the segment responsible for predicting

whether the instance is sampled from $P(X)$, and L_d denotes the log-likelihood of predicting the correct domain (i.e. which distribution was the point sampled from).

$$L_s = \mathbb{E}[\log(P(S = 1|X_0, F(X_t)))] + \mathbb{E}[\log(P(S = 0|G(F(X_t)), F(X_t)))] \quad (2)$$

$$L_d = \mathbb{E}[\log(P(D_l = d_l|X_0, F(X_t)))] + \mathbb{E}[\log(P(D_l = d_l|G(F(X_t)), F(X_t)))] \quad (3)$$

In Figure 1, I symbolizes the concatenated inputs supplied to D . The output of D can then be written as $D(I) = (P(S|I), P(D_l|I))$. The goal of D is to maximise $\mathcal{L}(G, D, F) = L_s + L_d$ while the goal of the G is to maximise $L_d - L_s$. G has two tasks: to fool D and produce outputs which are similar to the target distribution. Therefore, G needs to be penalised based on the distance (dissimilarity) between its output and target instances: $\mathcal{L}_{L1}(G) = \mathbb{E}_{X_0, X_t} [\|X_0 - G(F(X_t))\|_1]$.

The task of selecting the optimal generator G^* , can be expressed as follows:

$$G^* = \arg \min_G \max_D (\mathcal{L}(G, D, F) + \lambda \mathcal{L}_{L1}(G)) \quad (4)$$

Finally, let us consider the case of the label classifier LC and feature extractor F . Optimisation of LC follows the classic supervised learning paradigm, whereby LC aims to minimise its prediction loss $\mathcal{L}_{LC}(F, LC)$ by adjusting its parameters to accurately predict class labels based on features outputted by F . F is trained using \mathcal{L}_{LC} and \mathcal{L}_d . F aims to maximise LC 's accuracy while confusing D , ensuring the extracted features are generic and domain-invariant.

$$F^* = \arg \min_F \max_D (\mathcal{L}_{LC} - \lambda \cdot \mathcal{L}_{P(D_l=d_l|X_0, F(X_t))}) \quad (5)$$

To summarize the approach, during training, there are two adversarial two-player games. The first one involves the feature extractor F and the part of the discriminator D responsible for predicting the domain label, and the second one is the generator G vs. the discriminator D . For further clarity, Pseudocode for training GDAN can be found in Appendix A.

4 Experimental Setup

This section describes our process for evaluating GDAN. By leveraging two data-generators developed by Perdomo et al. [2] and Izzo et al. [20], we design a suite of experiments to compare the accuracy (performance) of GDAN against two benchmark models. We also describe how we evaluate GDAN's understanding of performative drift. Results from a baseline experiment has been included in Appendix 5 and a full list of the network architectures and experimental parameters used in this work have been included in the Supplementary Materials.

4.1 Simulation Design and Evaluation Metrics

To the best of our knowledge, there exists no publicly available dataset with known performative drift. We are therefore required to use the semi-real Perdomo [2] and synthetic Izzo [20] data generators. Additionally, our experiments require a dataset with ground truth labels, where each data point is associated with a specific distribution. These distributions are sequentially generated by inducing performative drift on the preceding one. For performance evaluation, access to the parameters of the drift-inducing model is mandatory.

A simulation run starts by generating data distribution X_0 using the chosen data generator. Then, a logistic regression model M_0 is trained on X_0 to establish performance benchmarks. M_0 's parameters are then given to the data generator, influencing the data distribution of future instances, simulating performative drift. Each iteration (t) represents a performative drift event. At each iteration, four models are evaluated:

1. M_0 : The original logistic regression model trained on data X_0 and evaluated on data X_i .
2. M_{ret} : A logistic regression model trained and evaluated on data X_i .
3. M_G : The original model M_0 evaluated on data generated by $G(F(X_t))$.
4. M_{LC} : GDAN's label classifier.

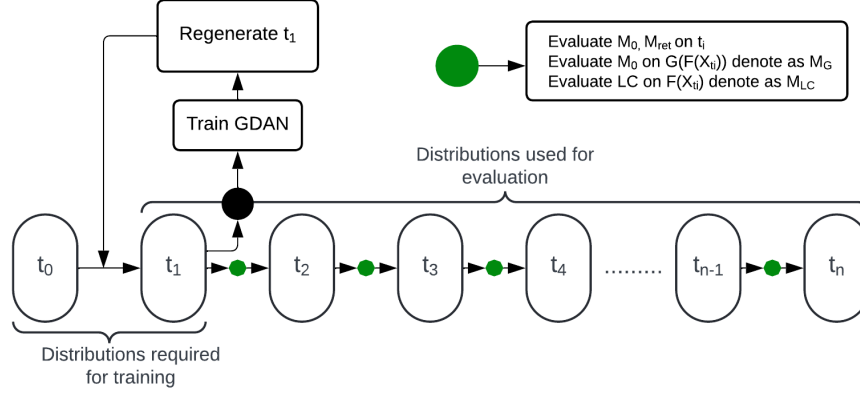


Figure 2: Visualization of the flow of the simulation. For training of the GDAN architecture, the only necessary distributions are annotated baseline $t = 0$ and the first distribution when drift is detected $t = 1$. Iterations $1 \dots n$ are used for evaluation purposes. After a model is trained, $t = 1$ is regenerated and the testing starts on it. In each iteration, four models are evaluated. The diagram depicts a division, which is similar to a test/train split in a classic ML setup.

At each iteration, prediction accuracy is recorded to ascertain the performance of each model. Additionally, The L_1 norm between X_0 and X_i is compared to the L_1 norm between X_0 and $G(F(X_i))$. As a simulation run progresses, performative drift causes X_i to look less like data distribution X_0 , which should be reflected in the L_1 norm. If GDAN successfully learned a domain-invariant representation of the incoming data, the L_1 norm between X_0 and $G(F(X_i))$ should remain as close to 0.0 as possible throughout the simulation run.

There is currently no framework for evaluating models in the performative setting. Thus, we treat the models M_0 and M_{ret} as our baselines with M_0 representing a lower-bound given that it undergoes no retraining, while M_{ret} acts like an upper-bound as it is continuously retrained after each drift event.

4.2 Data generation

4.2.1 Perdomo Generator

We implement a slightly modified version of the data generation process, described with the following equation.

$$x_{t+1} = x_t - \epsilon B \theta \quad (6)$$

θ symbolizes the feature coefficients of the logistic regression, B indexes whether the feature is performative, i.e. it gets influenced by the drift. And ϵ informs about the strength of the performativity. X_0 is created by loading the data from *GiveMeSomeCredit* dataset [21]. For this experiment, we test two setups. One where θ is changed by retraining every iteration (Dynamic Drift), and second when θ is constant from $t = 0$ (Monotonous Drift).

4.2.2 Izzo Generator

For this generator we also slightly change the scheme of data generation, as we move it from \mathbf{R} to \mathbf{R}^n . The main goal of this generator is to model a real-world spam detection situation, where only one class (the spammers) tries to modify their behaviour, to deceive the predictor.

$$x|y=0, \theta \sim \mathcal{N}(\mu_0, \sigma_0^2) \quad x|y=1, \theta \sim \mathcal{N}(f(\theta), \sigma_1^2) \quad (7)$$

The function of moving the average of the distribution can be described with the following equation, where n is the index of the feature.

$$\mu_{i,n} = f(\theta_n) = \mu_1 - \epsilon \cdot \theta_n \cdot B_n \quad (8)$$

5 Results and Discussion

Table 1 presents the results of the experiments with the Perdomo data generator. The accuracies of M_{LC} and M_G are competitive in earlier iterations. Later they start diverging from the baseline, which is more rapid in the case where the drift is dynamic. Given that GDAN is trained on only two distributions of data, it only learns to replicate one direction of drift. Performance is better when the drift is monotonous as the direction of drift is constant. In the dynamic case, the

Table 1: Summary of experiments with Perdomo generator. Each experiment has been performed 10 times, and each time we sample 10000 points from the data generator and evolve them by inducing drift. The values presented in the table are means and standard deviations.

Method	Metric	1	2	3	4	5	6	7	8	9	10
Monotonous Drift	Acc M_0	71.53 ± 0.285	71.04 ± 0.311	70.05 ± 0.291	68.92 ± 0.274	67.92 ± 0.285	66.91 ± 0.303	66.04 ± 0.329	65.13 ± 0.334	64.14 ± 0.327	63.22 ± 0.303
	Acc M_G	72.71 ± 0.268	72.26 ± 0.206	71.96 ± 0.178	71.88 ± 0.207	71.80 ± 0.180	71.56 ± 0.167	70.88 ± 0.142	70.06 ± 0.236	68.94 ± 0.249	67.53 ± 0.341
	Acc M_{LC}	76.02 ± 0.302	75.92 ± 0.279	74.91 ± 0.198	73.59 ± 0.203	71.91 ± 0.177	69.55 ± 0.209	66.63 ± 0.337	63.38 ± 0.273	59.94 ± 0.269	56.78 ± 0.286
	Acc M_{ret}	71.38 ± 1.480	71.38 ± 1.485	71.38 ± 1.481	71.38 ± 1.487	71.38 ± 1.482	71.38 ± 1.484	71.38 ± 1.480	71.38 ± 1.482	71.38 ± 1.489	71.38 ± 1.485
	$L_1(X_0, X_i)$	0.107 ± 0.000	0.213 ± 0.000	0.32 ± 0.000	0.427 ± 0.000	0.533 ± 0.000	0.64 ± 0.000	0.747 ± 0.000	0.853 ± 0.000	0.96 ± 0.000	1.067 ± 0.000
	$L_1(X_0, G(F(X_i)))$	0.112 ± 0.001	0.119 ± 0.001	0.136 ± 0.001	0.158 ± 0.001	0.182 ± 0.001	0.204 ± 0.001	0.226 ± 0.001	0.247 ± 0.001	0.266 ± 0.001	0.285 ± 0.001
Dynamic Drift	Acc M_0	71.79 ± 0.387	71.2 ± 0.431	70.17 ± 0.655	69.07 ± 0.774	68.52 ± 0.896	66.96 ± 0.953	66.04 ± 1.043	65.12 ± 1.252	64.19 ± 1.284	63.38 ± 1.255
	Acc M_G	72.8 ± 0.261	72.29 ± 0.420	71.89 ± 0.456	71.5 ± 0.474	70.71 ± 1.143	69.98 ± 1.874	69.3 ± 2.277	68.3 ± 2.672	67.05 ± 2.990	65.83 ± 3.292
	Acc M_{LC}	75.99 ± 0.264	75.35 ± 0.832	72.32 ± 3.793	68.34 ± 6.717	64.3 ± 8.599	60.97 ± 9.147	58.21 ± 9.122	55.59 ± 8.515	53.35 ± 7.729	51.62 ± 6.976
	Acc M_{ret}	72.29 ± 0.945	72.29 ± 0.945	72.29 ± 0.947	72.29 ± 0.947	72.29 ± 0.949	72.29 ± 0.947	72.29 ± 0.945	72.29 ± 0.938	72.29 ± 0.952	72.29 ± 0.944
	$L_1(X_0, X_i)$	0.107 ± 0.000	0.232 ± 0.022	0.36 ± 0.041	0.488 ± 0.061	0.616 ± 0.081	0.744 ± 0.010	0.872 ± 0.012	1.0 ± 0.141	1.128 ± 0.161	1.255 ± 0.180
	$L_1(X_0, G(F(X_i)))$	0.112 ± 0.001	0.127 ± 0.008	0.155 ± 0.015	0.186 ± 0.021	0.216 ± 0.025	0.245 ± 0.031	0.275 ± 0.037	0.304 ± 0.046	0.335 ± 0.055	0.367 ± 0.065

direction of the drift is not constant which makes GDAN’s task more complex. This is reflected in the larger standard deviations observed when the drift is dynamic. As the newly created distributions become increasingly different from the original distributions used for training, GDAN’s performance degrades. However, the accuracy of M_{LC} in the first five (monotonous), and first three (dynamic) iterations show that it is possible to train a classifier whose performance is superior to a retrained predictor. Additionally, the performance of M_G indicates that GDAN can create domain-invariant representations which are understandable by models only trained on data from $t = 0$ (e.g. M_0).

Considering the distance (L_1) metrics, it is noticeable that the data generator with dynamic performative drift produces data with greater dissimilarity from iteration $t = 0$ to $t = i$ when compared to the data generator with monotonous performative drift. Additionally, GDAN’s reconstructed distributions $G(F(X_i))$ are always closer to the original distribution X_0 , indicating an ability to reverse the distribution shifts caused by the performative drift.

These results demonstrate one of the key characteristics of performative drift. Whenever a model is retrained, the performative drift’s behaviour changes too. Retraining is a commonplace solution for handling intrinsic drift. Our results suggest that retraining would work in the performative setting if the deployed model has unfettered access to the labels of the instances it predicts on. If that is not case, our results indicate that less frequent retraining with a greater focus on drift understanding and drift reversal (using GDAN for example) may reduce the rate of performance degradation (See M_g compared to M_0 in Table 1 for example). This is because fewer retraining steps would provide more monotonous performative drift which our results clearly show is easier to manage.

Table 2: Summary of experiments with Izzo data generator (20k datapoints sampled, averaged over 20 runs). M_{LC} and M_{ret} are excluded, as both achieve perfect accuracy. All values oscillate with the retraining of the logistic regressor (every 3 iterations), demonstrating the cyclic nature of the performative drift.

Metric/iter	1	2	3	4	5	6	7	8	9	10
Acc M_0	50.3 ± 0.535	50.21 ± 0.295	50.02 ± 0.349	50.21 ± 0.449	60.03 ± 19.98	60.11 ± 19.95	59.88 ± 20.06	49.99 ± 0.372	50.21 ± 0.436	49.94 ± 0.431
Acc M_G	78.59 ± 18.36	78.52 ± 18.34	78.63 ± 18.28	78.63 ± 18.21	94.33 ± 12.54	94.47 ± 12.26	94.24 ± 12.74	77.12 ± 18.72	77.07 ± 18.78	77.17 ± 18.68
$L_1(X_0, X_i)$	3.78 ± 0.065	3.78 ± 0.068	3.78 ± 0.065	3.78 ± 0.066	3.67 ± 0.143	3.67 ± 0.138	3.66 ± 0.142	3.82 ± 0.096	3.82 ± 0.090	3.82 ± 0.091
$L_1(X_0, G(F(X_i)))$	3.39 ± 0.024	3.39 ± 0.017	3.39 ± 0.014	3.39 ± 0.012	3.41 ± 0.028	3.39 ± 0.026	3.39 ± 0.014	3.4 ± 0.042	3.4 ± 0.031	3.39 ± 0.030
Metric/iter	11	12	13	14	15	16	17	18	19	20
Acc M_0	65.1 ± 22.76	64.88 ± 22.91	64.73 ± 23.01	49.83 ± 0.700	50.15 ± 0.650	50.14 ± 0.287	63.66 ± 21.06	63.74 ± 21.10	63.57 ± 21.13	50.13 ± 0.289
Acc M_G	96.42 ± 10.73	96.32 ± 11.02	96.35 ± 10.94	76.07 ± 19.05	76.57 ± 18.68	76.44 ± 18.78	99.56 ± 1.070	99.53 ± 1.149	99.56 ± 1.033	74.54 ± 17.57
$L_1(X_0, X_i)$	3.67 ± 0.133	3.67 ± 0.132	3.68 ± 0.134	3.79 ± 0.030	3.79 ± 0.033	3.79 ± 0.035	3.68 ± 0.139	3.69 ± 0.137	3.69 ± 0.130	3.79 ± 0.037
$L_1(X_0, G(F(X_i)))$	3.38 ± 0.021	3.38 ± 0.021	3.39 ± 0.019	3.39 ± 0.019	3.39 ± 0.019	3.38 ± 0.026	3.38 ± 0.019	3.38 ± 0.036	3.39 ± 0.024	3.39 ± 0.015

Table 2 presents the results of the Izzo experiments. Interestingly, the nature of the Izzo generator’s drift is cyclic. This can be seen by the oscillation of M_0 and M_G ’s accuracies every three iterations. Additionally, the original logistic regression achieves greater accuracy on the mapped representations generated by GDAN (M_G). This indicates that despite GDAN’s inability to completely minimize the dissimilarity of the drifted data points, GDAN is still capable of providing drift resistant classification. This is further supported by GDAN’s label classifier which achieved perfect accuracy across all simulation runs.

Figures 3a and 3b illustrate how GDAN acts on the performative features of the Perdomo data generator. The generated density region (green) does not overlap perfectly with the original one (red). However, GDAN’s generator projects the mean of each distribution correctly. Despite GDAN’s struggles to replicate outliers, the centres of the green and red density regions remain relatively close, suggesting alignment of central tendencies. A slight degradation occurs over the course of a simulation run, which is visible when analysing feature 8 where two spikes are visible on the green curve at iteration 0, while this same area is more uniform at iteration 9. This explains the decrease in performance observed for both the M_{LC} and M_G (Table 1) models.

Figure 4 presents the evolution of the PCA clusters in the Izzo experiment where the blue (drifted) clusters oscillate between the red (original) ones. Indicated by the inconsistent resemblance of the green (generated) clusters to the original (red) clusters, this oscillatory phenomena of the Izzo data generator impacts the results of GDAN’s generator. This is because GDAN is only trained over a single iteration, making it incapable of understanding, and reversing the effects of multi-iteration drift phenomena.

5.1 Sensitivity of Dataset Size

Tables 3 and 4 present the results of additional experiments conducted to ascertain GDAN’s sensitivity to the size of the training set. The experiment using the Perdomo generator demonstrated that a reduction in training data size negatively

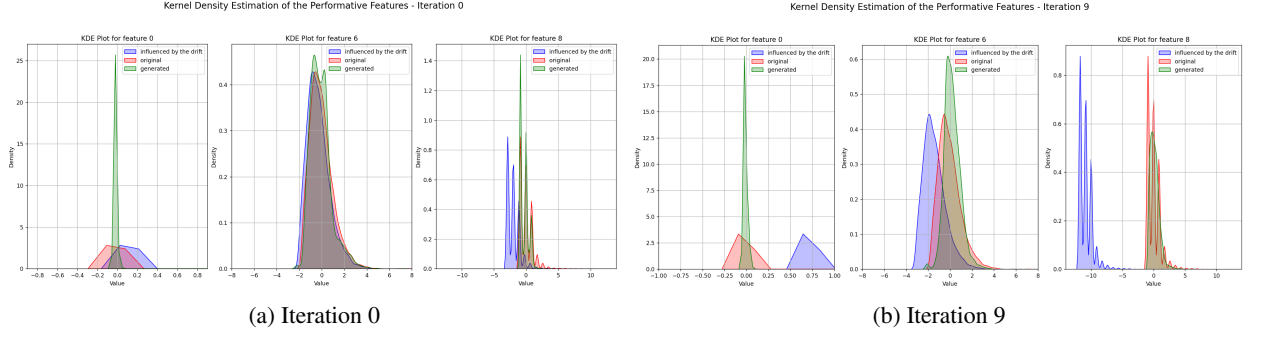


Figure 3: Kernel Density Estimation of the Perdomo data generator’s performative features. Using GDAN, the blue (drifted) data points are projected back to the red (original) data distribution. These projections are indicated by the green areas which show that GDAN is capable of reversing the effects of the drift, despite not being able to recreate the shape of the original distribution exactly.

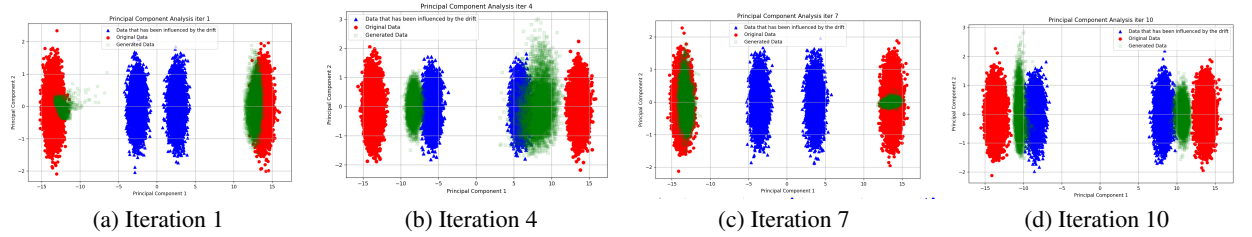


Figure 4: PCA visualization of the Izzo data generator on iterations where the logistic regressor was retrained. The figure illustrates the cyclical nature of the drift, as the blue (drifted) clusters oscillate, moving to and from the stationary red (original data distribution) clusters. This dynamic significantly affects GDAN’s ability to project the drifted data points as shown by the green clusters.

affects accuracy metrics. Models trained on $5k$ and $10k$ samples perform worse and performance decays more rapidly. With fewer data points, GDAN struggles to create a domain-invariant representation, which is visible when comparing the accuracies of M_{LC} . A spike in the performance of M_{LC} is observed when GDAN is trained on $10k$ samples. This spike is temporary and arises because the model fails to learn the correct direction of drift for one of the performative features (feature 6). The results of the Izzo generator are more straightforward. The original results (Table 2) were obtained using a model trained on $20k$ samples. The results in Table 4 are inferior to those. The model trained on $5k$ data points achieves an accuracy marginally above random guessing, indicating severe underfitting. The model trained on $40k$ data points exhibits clear signs of overfitting, failing to generalize effectively on drifted distributions. Overall, these results show that GDAN, like most ML-models, is susceptible to performance degradation as the number of training samples tends to zero.

6 Conclusions and Future Work

In this work we addressed the problem of performance degradation in settings with performative concept drift. That is, scenarios where a model’s predictions influence the data it must later predict on. We developed GDAN, a novel architecture that combines Generative and Domain Adversarial Neural Networks. By creating domain-invariant representations of incoming data, GDAN is able to reverse the effects of performative drift and enable stable classification. Empirically evaluating GDAN on the Perdomo [2] and Izzo [20] data generators, results indicated that GDAN performs sufficiently well, consistently outperforming baseline models trained under the same conditions. Our results also indicated GDAN’s performance degrades in scenarios where the direction of performative drift changes frequently. In such scenarios, GDAN can be inferior to simple retraining regimes. However, there are cases where retraining is not feasible, such as when new labels arrive with delay. We also showed that GDAN can model the direction of performative drift, and reverse its effects. This allows GDAN to provide deeper insights into the nature of performative drift, and allows other models to leverage GDAN to make themselves drift-resistant. Future work will aim to use real-world data to validate GDAN’s performance as the data generators used in this work only approximate real-world phenomena.

Table 3: Results of varying dataset sizes with the Perdomo data generator. In general, GDAN performs is incapable of creating a domain-invariant (drift-resistant) representation of the data with fewer training samples.

No. data points	Metric	1	2	3	4	5	6	7	8	9	10
5k	Acc M_g	71.65 ± 0.35	71.67 ± 0.45	71.45 ± 0.44	70.98 ± 1.20	70.08 ± 1.77	68.58 ± 1.97	66.62 ± 2.00	65.05 ± 1.71	63.62 ± 1.93	62.18 ± 3.12
	Acc M_{LC}	61.16 ± 0.44	60.74 ± 0.47	60.47 ± 0.55	60.36 ± 0.65	60.54 ± 0.97	60.84 ± 1.33	60.80 ± 1.50	60.74 ± 1.58	60.69 ± 1.49	60.34 ± 1.58
10k	Acc M_g	71.61 ± 0.15	71.05 ± 0.41	69.88 ± 0.55	68.25 ± 0.71	66.38 ± 1.09	64.41 ± 1.68	62.64 ± 1.93	61.01 ± 1.92	59.81 ± 2.01	58.75 ± 2.04
	Acc M_{LC}	62.47 ± 0.21	62.82 ± 0.33	63.41 ± 0.41	63.74 ± 0.40	64.16 ± 0.55	65.02 ± 0.85	66.27 ± 1.17	67.52 ± 1.52	68.50 ± 1.59	69.26 ± 1.67

Table 4: Results of varying dataset sizes with the Izzo data generator. In both cases, GDAN’s performance is inferior exhibiting both over (40k) and underfitting (5k). M_{LC} and M_{ret} are omitted as they achieve perfect scores.

No. data points	Metric/iter	1	2	3	4	5	6	7	8	9	10
5k	Acc M_0	50.01 ± 0.490	49.91 ± 0.350	49.76 ± 0.570	50.03 ± 0.570	54.92 ± 15.03	54.96 ± 15.02	54.81 ± 15.07	49.94 ± 0.400	50.14 ± 0.540	49.94 ± 0.420
	Acc M_g	50.01 ± 0.490	49.91 ± 0.350	49.76 ± 0.570	50.03 ± 0.570	57.84 ± 16.73	57.85 ± 16.75	57.75 ± 16.77	49.95 ± 0.400	50.14 ± 0.540	49.94 ± 0.420
40k	Acc M_0	49.95 ± 0.580	49.99 ± 0.520	49.91 ± 0.510	49.84 ± 0.470	55.86 ± 15.32	55.79 ± 15.32	56.10 ± 15.21	50.00 ± 0.480	49.98 ± 0.460	50.00 ± 0.390
	Acc M_g	68.10 ± 10.95	68.25 ± 10.92	68.09 ± 10.85	68.16 ± 10.96	58.76 ± 18.26	58.75 ± 18.28	59.02 ± 18.14	68.63 ± 10.89	68.75 ± 10.90	68.80 ± 10.89

Furthermore, this work only investigated scenarios with performative drift whereas real world settings may have both performative and traditional (intrinsic) concept drift. Extending GDAN to include performative drift detection methods [22] would also be beneficial. This would address one the strongest assumptions in Performative Prediction literature which is that the presence of performative drift is known beforehand. Lastly, performative drift does not behave like intrinsic drift. Unlike intrinsic drift, the volatility of performative drift is tied to the rate at which deployed predictors are updated. Our results show that in settings that are performative, incremental learning strategies may be less effective as they result in more volatile drift phenomena. Future work will examine these claims in greater detail and seek to propose alternative learning strategies.

References

- [1] João Gama, Indrė Žliobaitė, Albert Bifet, Mykola Pechenizkiy, and Hamid Bouchachia. A survey on concept drift adaptation. *ACM Computing Surveys (CSUR)*, 46, 2014.
- [2] Juan Perdomo, Tijana Zrnic, Celestine Mendler-Dünner, and Moritz Hardt. Performative prediction. In Hal Daumé III and Aarti Singh, editors, *Proceedings of the 37th International Conference on Machine Learning*, volume 119, pages 7599–7609. PMLR, 2020.
- [3] S. Hoi, Doyen Sahoo, Jing Lu, and P. Zhao. Online learning: A comprehensive survey. *Neurocomputing*, 459:249–289, 2018.
- [4] Georg Kreml, Vera Hofer, Geoffrey Webb, and Eyke Hüllermeier. Beyond adaptation: Understanding distributional changes (Dagstuhl Seminar 20372). In *Dagstuhl Reports*, volume 10. Schloss Dagstuhl-Leibniz-Zentrum für Informatik, 2021.
- [5] Yaroslav Ganin, Evgeniya Ustinova, Hana Ajakan, Pascal Germain, Hugo Larochelle, François Laviolette, Mario March, and Victor Lempitsky. Domain-adversarial training of neural networks. *Journal of Machine Learning Research*, 17(59):1–35, 2016.

- [6] Antonia Creswell, Tom White, Vincent Dumoulin, Kai Arulkumaran, Biswa Sengupta, and Anil A. Bharath. Generative adversarial networks: An overview. *Signal Processing Magazine*, 35(1):53–65, 2018.
- [7] Ian Goodfellow, Jean Pouget-Abadie, Mehdi Mirza, Bing Xu, David Warde-Farley, Sherjil Ozair, Aaron Courville, and Yoshua Bengio. Generative adversarial nets. *Advances in neural information processing systems*, 27, 2014.
- [8] Georg Kreml, David Bodnar, and Anita Hrubos. When learning indeed changes the world: Diagnosing prediction-induced drift. In Tijl De Bie, Elisa Fromont, and Matthijs van Leeuwen, editors, *Advances in Intelligent Data Analysis XIV*, volume 9385 of *LNCS*. Springer, 2015.
- [9] Masoud Mansoury, Himan Abdollahpouri, Mykola Pechenizkiy, Bamshad Mobasher, and Robin Burke. Feedback loop and bias amplification in recommender systems. In *Proceedings of the 29th ACM international conference on information & knowledge management*, pages 2145–2148, 2020.
- [10] Jiawei Chen, Hande Dong, Xiang Wang, Fuli Feng, Meng Wang, and Xiangnan He. Bias and debias in recommender system: A survey and future directions. *Transactions on Information Systems*, 41(3):1–39, 2023.
- [11] Robert Epstein, Yunyi Huang, Miles Megerdooimian, and Vanessa R Zankich. The “opinion matching effect”(ome): A subtle but powerful new form of influence that is apparently being used on the internet. *PloS One*, 19(9):e0309897, 2024.
- [12] Omri Ben-Eliezer, Rajesh Jayaram, David P Woodruff, and Eylon Yogev. A framework for adversarially robust streaming algorithms. *Journal of the ACM (JACM)*, 69(2):1–33, 2022.
- [13] Łukasz Korycki and Bartosz Krawczyk. Adversarial concept drift detection under poisoning attacks for robust data stream mining. *Machine Learning*, 113(5):3303–3304, 2024.
- [14] Tianjiao Luo, Ziyu Zhu, Jianfei Chen, and Jun Zhu. Stabilizing gans’ training with brownian motion controller. In *International Conference on Machine Learning*, pages 23140–23156. PMLR, 2023.
- [15] Naveen Kodali, Jacob D. Abernethy, James Hays, and Z. Kira. How to train your DRAGAN. *ArXiv*, abs/1705.07215, 2017.
- [16] Mehdi Mirza and Simon Osindero. Conditional generative adversarial nets. *arXiv preprint arXiv:1411.1784*, 2014.
- [17] Augustus Odena, Christopher Olah, and Jonathon Shlens. Conditional image synthesis with auxiliary classifier GANs. In Doina Precup and Yee Whye Teh, editors, *Proceedings of the 34th International Conference on Machine Learning*, volume 70, pages 2642–2651. PMLR, 2017.
- [18] Phillip Isola, Jun-Yan Zhu, Tinghui Zhou, and Alexei A. Efros. Image-to-image translation with conditional adversarial networks. 2018.
- [19] Deepak Pathak, Philipp Krahenbuhl, Jeff Donahue, Trevor Darrell, and Alexei A Efros. Context encoders: Feature learning by inpainting. In *Proceedings of the IEEE conference on computer vision and pattern recognition*, pages 2536–2544, 2016.
- [20] Zachary Izzo, James Zou, and Lexing Ying. How to learn when data gradually reacts to your model. In *International Conference on Artificial Intelligence and Statistics*, pages 3998–4035. PMLR, 2022.
- [21] Credit Fusion and Will Cukierski. Give me some credit, 2011.
- [22] Brandon Gower-Winter, Georg Kreml, Sergey Dragomiretskiy, Tineke Jelsma, and Arno Siebes. Identifying predictions that influence the future: Detecting performative concept drift in data streams. In *Proceedings of the AAAI Conference on Artificial Intelligence*, 2025.

A Training GDAN

Algorithm 1 highlights the process of training GDAN. θ denotes the weights of a model, with the subscript indicating the specific model. The parameter μ is the model specific learning rate. λ_1 and λ_2 are regularisation parameters, which control the degree of penalisation a model receives. The exact values for training GDAN in this work are included in the Supplementary Materials.

Table 5: Baseline experiment whereby data is influenced once and then continuously sampled from distribution t_1 . In this scenario, no deterioration occurs and the performance of M_{LC} and M_g are superior to the accuracies achieved by M_0 and M_{ret} . This experiment serves as a sanity check for our proposed solution.

Metric	1	2	3	4	5	6	7	8	9	10
Acc M_0	71.62 ± 0.23	71.62 ± 0.23	71.62 ± 0.23	71.62 ± 0.23	71.62 ± 0.23	71.62 ± 0.23	71.62 ± 0.23	71.62 ± 0.23	71.62 ± 0.23	71.62 ± 0.23
Acc M_{ret}	70.69 ± 0.98	70.69 ± 0.98	70.69 ± 0.98	70.69 ± 0.98	70.69 ± 0.98	70.69 ± 0.98	70.69 ± 0.98	70.69 ± 0.98	70.69 ± 0.98	70.69 ± 0.98
Acc M_g	72.76 ± 0.20	72.76 ± 0.20	72.76 ± 0.20	72.76 ± 0.20	72.76 ± 0.20	72.76 ± 0.20	72.76 ± 0.20	72.76 ± 0.20	72.76 ± 0.20	72.76 ± 0.20
Acc M_{LC}	76.00 ± 0.20	76.00 ± 0.20	76.00 ± 0.20	76.00 ± 0.20	76.00 ± 0.20	76.00 ± 0.20	76.00 ± 0.20	76.00 ± 0.20	76.00 ± 0.20	76.00 ± 0.20
$L_1(X_0, X_i)$	0.107 ± 0.000	0.107 ± 0.000	0.107 ± 0.000	0.107 ± 0.000	0.107 ± 0.000	0.107 ± 0.000	0.107 ± 0.000	0.107 ± 0.000	0.107 ± 0.000	0.107 ± 0.000
$L_1(X_0, G(F(X_i)))$	0.112 ± 0.001	0.112 ± 0.001	0.112 ± 0.001	0.112 ± 0.001	0.112 ± 0.001	0.112 ± 0.001	0.112 ± 0.001	0.112 ± 0.001	0.112 ± 0.001	0.112 ± 0.001

Algorithm 1 Gradient Descent Training of GDAN

Input: Training iterations N , batch size m and k (the number of steps after which the generator starts to be updated and the feature extractor stops being updated)

Create $Z = X_0 \cup X_1$ with class labels C and domain labels D_l

for number of training iterations **do**

- Sample minibatch of $\frac{m}{2}m$ examples $\{x^{(1)}, \dots, x^{(\frac{m}{2})}\}$ from Z
- Arbitrarily pair each sample with a point from distribution X_0
- Pass each sample through the network components and record their outputs.
- Generate another minibatch of $\frac{m}{2}$ samples by using the generator with $F(x^{(\frac{m}{2})})$ as input, and assign domain labels. The generator loss will only be calculated based on these generated instances (later denoted as m_1). The discriminator is trained on both real and generated samples.
- Calculate loss functions.
 - Update F , LC , D , and G :

$$\begin{aligned}
\theta_F &\leftarrow \theta_F - \mu_F(\nabla_{\theta_F} \mathcal{L}_{LC}^m - \lambda_1 \nabla_{\theta_F} \mathcal{L}_{domain}^{\frac{1}{2}m}) \\
\theta_{LC} &\leftarrow \theta_{LC} - \mu_{LC} \nabla_{\theta_{LC}} \mathcal{L}_{LC}^m \\
\theta_D &\leftarrow \theta_D - \mu_D \nabla_{\theta_D} (\mathcal{L}_{source}^m + \mathcal{L}_{domain}^m) \\
\theta_G &\leftarrow \theta_G - \mu_G \nabla_{\theta_G} (\mathcal{L}_{domain}^{m_1} + \mathcal{L}_{source}^{m_1} + \lambda_2 \mathcal{L}_{L1})
\end{aligned}$$

end for

Output: Trained F , LC , G , and D
